

*This research was supported by the Advanced Research Projects Agency of the Department of Defense and was monitored by the U. S. Army Research Office-Durham under Contract DA-31-124-ARO-D-257.

†Permanent address: Department of Theoretical Physics, The Hebrew University, Jerusalem, Israel.

¹C. L. Pekeris, *Phys. Rev.* **126**, 1470 (1962).

²K. Frankowski and C. L. Pekeris, *Phys. Rev.* **146**, 46 (1966).

³L. R. Henrich, *Astrophys. J.* **99**, 59 (1943).

⁴J. F. Hart and G. Herzberg, *Phys. Rev.* **106**, 79 (1957).

⁵K. T. Chung and R. P. Hurst, *Phys. Rev.* **152**, 35 (1966).

⁶T. Ohmura and H. Ohmura, *Phys. Rev.* **118**, 154 (1960).

⁷The work of Burke and Taylor, in which correlation terms were added to a close-coupling calculation, could actually represent an added step of sophistication to the work presented here. However, in order to test their numerical procedure, they calculate the binding energy of the ¹S state of H⁻. They report their results when 16

correlation terms are used (0.027 64 a. u.) which is slightly inferior to our results with only seven Hylleraas terms (0.027 648 a. u.). The cause for this discrepancy is unknown to us. P. G. Burke and A. J. Taylor, *Proc. Roy. Soc. (London)* **88**, 549 (1966).

⁸M. Inokuti and Y. -K. Kim, *Phys. Rev.* **173**, 154 (1968).

⁹F. H. Gertler, H. B. Snodgrass, and L. Spruch, *Phys. Rev.* **172**, 110 (1968); A. A. Frost, M. Inokuti and J. P. Lowe, *J. Chem. Phys.* **41**, 482 (1964). In this paper the mass of the positron was changed but no attempt was made to extrapolate.

¹⁰The factor $m^{1/2}$ is actually second order in $(m - m_0)$ but was included in order to rectify the data of Table IV (see Fig. 1). This second order behavior is confirmed by a square-well calculation.

¹¹C. Schwartz, *Phys. Rev.* **124**, 1468 (1961); R. J. Drachman, *ibid.* **173**, 190 (1968).

¹²R. J. Drachman, *Phys. Rev.* **171**, 110 (1968).

¹³The material presented in this Appendix will also appear in a Ph.D. thesis by N. Minsky, Department of Physics, The Hebrew University, Jerusalem, Israel.

Elastic Scattering of 145-, 279-, 412-, and 662-keV γ Rays from Lead*

M. Schumacher†

Bartol Research Foundation of the Franklin Institute, Swarthmore, Pennsylvania

(Received 31 January 1969)

The differential cross section for elastic scattering of 145-, 279-, 412-, and 662-keV γ rays from lead has been measured in the angle interval 30 to 150° using a lithium-drifted germanium detector. The experimental results are in general agreement with the theory of Brown *et al.* Approximative formulas for the differential cross section of Rayleigh scattering are discussed.

I. INTRODUCTION

The good energy resolution of lithium-drifted germanium detectors lead to an enormous increase in the accuracy of many experiments in γ -ray spectrometry. One of these experiments is the determination of the differential cross section for elastic scattering of γ rays which requires the separation of the elastic- and inelastic-scattering components. The elastic scattering is composed of four different processes: Rayleigh scattering, nuclear Thomson scattering, nuclear-resonance scattering, and Delbrück scattering. Of these four processes the Delbrück scattering is by far the most interesting one since

it yields in addition to the Lamb shift an information about the vacuum polarization. Unfortunately this process is also the weakest one, so that its contribution to the cross section can only be detected when the competing processes are very well known. This is one reason for being interested in an accurate determination of the differential cross section for Rayleigh scattering.

An exact calculation of the differential cross section for Rayleigh scattering has been carried out by Brown *et al.*¹⁻⁴ for the *K* electrons of mercury and the γ -ray energies 163, 327, 654, and 1308 keV. The main purpose of the present work was to check these calculated cross sections experimentally. For this reason the ex-

periment was performed with lead as the scattering material and with γ rays of 145-, 279-, 412-, and 662-keV energy. We decided not to perform an experiment at 1332 keV because of a recent measurement carried out with a germanium detector at this energy by Dixon and Storey.⁵

The method of Brown *et al.*¹⁻⁴ requires an extended calculation with a computer which has not been carried out for charge numbers other than 80. A further aim of this work therefore was to check the existing approximative calculations of differential cross sections for Rayleigh scattering. These calculations are of considerable interest to nuclear-resonance fluorescence experiments for which Rayleigh scattering is a troublesome companion.

II. EXPERIMENTAL METHOD AND RESULTS

The experiments were performed with sources of Ce^{141} (20 mCi), Hg^{203} (25 mCi), Au^{198} (50 mCi), and Cs^{137} (50 mCi) which essentially emit γ rays of a single energy. Most of the former experiments⁵ have been carried out with source strengths of many curies. The sources used in the present experiment were relatively weak. In spite of this fact relatively high counting rates were obtained so that after a run of a few hours the statistical error of the measured cross section was smaller than 2%. This was achieved in the following way: The Ge (Li) detector (Fig. 1) had a volume of 30 cc and a resolution of about 3.5 keV. By using Mallory 2000 as the shielding material, rather compact geometries were obtained with a distance of 23 cm between detector and scatterer and a distance of 12 cm between source and scatterer. Lead absorbers were placed in front of the detector in order to reduce the high counting rates at small energies.

The scatterers had the dimensions 1.50×2.25 in. and thicknesses of 0.145, 0.903, and 1.804

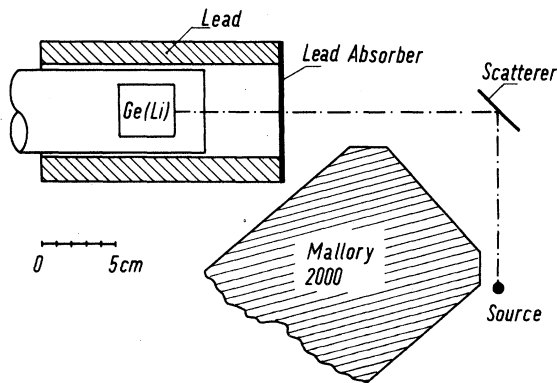


FIG. 1. Experimental configuration used for the energy $E_\gamma = \text{keV}$ and the scattering angle $\theta = 90^\circ$.

g/cm^2 for the experiments with the 145-, 279-, and 412-keV γ -ray energies, respectively. In the case of the 662-keV radiation the scatterer thickness was varied between 0.903 and 5.41 g/cm^2 in order to check the evaluation of the data. Great care was taken to make sure that the counting rate detected in the full-energy line was only due to elastic scattering from the scatterer. For this reason the background was subtracted from each of the obtained spectra. In addition, runs with an Al-comparison scatterer were carried out showing only the inelastically scattered line as one should expect from the smallness of the cross section for elastic scattering.

A certain difficulty arising in experiments with a germanium detector is the length of the electronic pulses which easily leads to a decrease of the counting-rate detected in a narrow line due to pile up. This decrease of the counting rate was measured with an electronic pulser showing that it was negligible in most cases. In some cases the decrease had to be taken into account by a small correction to the number of counts in the full-energy line.

Figure 2 shows some typical spectra which demonstrate the good separation of the elastically and the inelastically scattered lines even at small scattering angles. In addition they show the rapid increase of the cross section for elastic scattering in comparison to the cross section for Compton scattering with decreasing energy. The variation of the over-all detection efficiency is not larger than a factor 1.5 over each of the energy regions displayed in Fig. 2.

Figure 3 shows some of the spectra measured with the 279-keV γ radiation. The dots represent the spectra obtained with the lead scatterer consisting of the Rayleigh scattered line and the Compton scattered line. The solid lines underneath the dotted Compton lines represent the spectra obtained with an Al scatterer under the same geometrical conditions, normalized at the maximum. The Compton spectra from the Al and the Pb scatterers show a significant dissimilarity. The Compton spectra from the Pb scatterer are broader. In addition there is a continuum between the Compton scattered line and the elastically scattered line. This continuum cannot be explained as being due to pile up, since the probability for pile up was small according to the measurement with the pulser mentioned above. From the spectrum of the directly measured γ rays in Fig. 3 it can be seen that the low-energy part of the spectrum of the elastically scattered radiation also cannot account for the continuum. An estimate shows that bremsstrahlung produced by recoil electrons in the scatterer and multiple Compton scattering are not intense enough to account for the observed counting rate

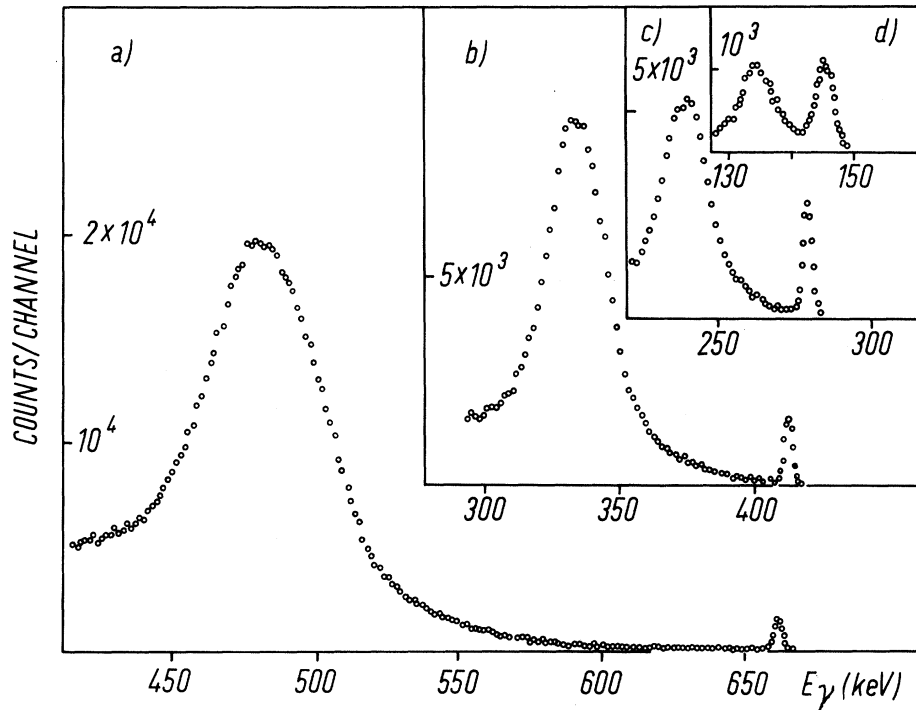


FIG. 2. Spectra of γ radiation scattered from lead under a scattering angle of 45° . The energies of the incident γ rays are (a) 662, (b) 412, (c) 279, and (d) 145 keV.

in the continuum, though they might give a contribution to it. Therefore it has to be concluded that most of the broadening and the continuum is due to the binding of the scattering electrons, an effect which is well known in the spectrometry of x rays.⁶ Bound electrons have a large momentum which leads to a Doppler broadening of the energy of the scattered quanta. The continuum can be explained as being due to a reduction of the Compton shift because of a partial momentum transfer from the electron to the nucleus. A similar observation has been made by Standing and Jovanovich⁷ who measured the spectra of Co^{60} γ rays scattered by different materials. Randles⁸ has calculated the differential cross section for incoherent scattering from K electrons on the basis of the theory of Brown *et al.*^{1,2} Neglecting the binding of the electrons in the intermediate state he obtains an expression which allows a numerical calculation of the spectra of the incoherently scattered quanta. The spectra in Fig. 3 cannot be explained without considering also the inelastic scattering from higher shells. Since our interest was mainly focused on an accurate determination of the differential cross section for elastic scattering and since the experiment probably can be improved with respect to the spectra of the inelastically scattered quanta we did not attempt a quantitative explanation of our spectra.

For the determination of the differential cross section for elastic scattering from the measured

counting rates, a computer program was used which calculated the contributions to the counting rate arising from the different volume elements of the scatterer. This calculation had to take into account the absorption of γ rays in the scatterer. The corresponding effective cross section σ_{abs} is the sum of the cross sections for photo effect, Compton effect, and Rayleigh scattering. In addition to the absorption, the double Rayleigh scattering had to be taken into account since it contributes a few percent to the counting rate of the elastically scattered radiation. Because of the strong forward peaking of the Rayleigh scattered radiation the double Rayleigh scattering can approximately be included in the calculation of the differential cross section by omitting the contribution of the Rayleigh scattering to σ_{abs} . A deviation from this approximation can only be expected at small scattering angles. A detailed estimate showed, however, that even at $\theta = 30^\circ$ this approximation is sufficiently accurate.

The evaluation of the differential cross sections requires an accurate value for the sum of the attenuation coefficients due to photo effect and Compton effect. This quantity can be obtained from a simple absorption experiment, if the absorber is thin and is placed at a large distance from the detector. In this case the attenuation of the beam due to Rayleigh scattering is compensated to a good approximation by the radiation scattered into the detector by neighboring

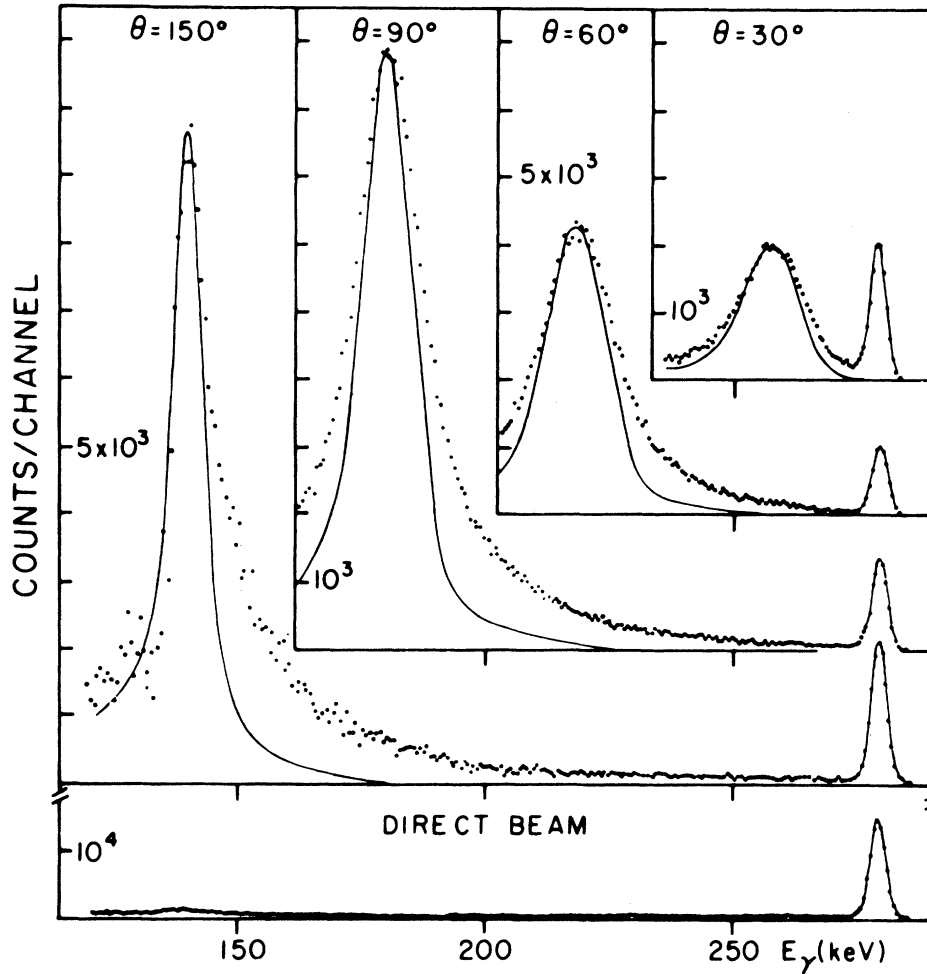


FIG. 3. Spectra of scattered γ radiation for different scattering angles. The energy of the incident γ ray is 279 keV. The dots represent the spectra obtained with a lead scatterer, the solid curves underneath the Compton peaks represent the spectra obtained with an aluminium comparison scatterer.

parts of the absorber. We obtained $\mu/\rho = 2.07$, 0.445, 0.205, and 0.1015 cm^2/g for the energies 145, 279, 412, and 662 keV, respectively.

Because of the finite sizes of the scatterers and the detector, the differential cross sections obtained in the way described above are averages over angular intervals which, for the geometries used, amounted to about 8° . From these average differential cross sections the slightly different

differential cross sections at the average scattering angles were calculated and listed in Table I.

III. ELASTIC-SCATTERING CALCULATIONS

The elastic scattering consists of the four components nuclear-resonance scattering, Delbrück scattering, Rayleigh scattering, and nuclear Thomson scattering.

TABLE I. Differential cross section for elastic scattering from lead.

Scattering angle θ (deg)	145 keV $d\sigma/d\Omega$ (cm^2/sr)	279 keV $d\sigma/d\Omega$ (cm^2/sr)	412 keV $d\sigma/d\Omega$ (cm^2/sr)	662 keV $d\sigma/d\Omega$ (cm^2/sr)
32	$(5.9 \pm 0.5) \times 10^{-24}$	$(1.12 \pm 0.09) \times 10^{-24}$	$(3.3 \pm 0.2) \times 10^{-25}$	$(5.7 \pm 0.5) \times 10^{-26}$
45	$(2.07 \pm 0.14) \times 10^{-24}$	$(4.0 \pm 0.3) \times 10^{-25}$	$(8.4 \pm 0.6) \times 10^{-26}$	$(2.12 \pm 0.15) \times 10^{-26}$
60	$(9.6 \pm 0.6) \times 10^{-25}$	$(1.30 \pm 0.08) \times 10^{-25}$	$(3.7 \pm 0.2) \times 10^{-26}$	$(8.0 \pm 0.5) \times 10^{-27}$
75	$(5.6 \pm 0.3) \times 10^{-25}$	$(5.9 \pm 0.3) \times 10^{-26}$	$(2.2 \pm 0.1) \times 10^{-26}$	$(3.7 \pm 0.2) \times 10^{-27}$
90	$(3.63 \pm 0.14) \times 10^{-25}$	$(4.4 \pm 0.2) \times 10^{-26}$	$(1.62 \pm 0.06) \times 10^{-26}$	$(2.38 \pm 0.09) \times 10^{-27}$
105	$(2.81 \pm 0.10) \times 10^{-25}$	$(4.15 \pm 0.17) \times 10^{-26}$	$(1.42 \pm 0.06) \times 10^{-26}$	$(1.98 \pm 0.08) \times 10^{-27}$
120	$(2.51 \pm 0.10) \times 10^{-25}$	$(4.13 \pm 0.17) \times 10^{-26}$	$(1.32 \pm 0.05) \times 10^{-26}$	$(1.78 \pm 0.07) \times 10^{-27}$
135	$(2.52 \pm 0.10) \times 10^{-25}$	$(4.29 \pm 0.17) \times 10^{-26}$	$(1.31 \pm 0.05) \times 10^{-26}$	$(1.67 \pm 0.07) \times 10^{-27}$
150	$(2.56 \pm 0.10) \times 10^{-25}$	$(4.37 \pm 0.17) \times 10^{-26}$	$(1.28 \pm 0.05) \times 10^{-26}$	$(1.58 \pm 0.07) \times 10^{-27}$

The nuclear-resonance scattering of γ rays with an energy of a few MeV is mainly due to the "tails" of the resonance curves of the nuclear levels at 15 to 20 MeV. Levinger⁹ has calculated the differential cross section for resonance scattering under these conditions showing that the contribution to the total scattering cross section is negligible for the energies of the present experiment.

A quantitative calculation of the amplitudes for Delbrück scattering has been published by Ehlitzky and Sheppy¹⁰ for energies between 1.3 and 16 MeV and angles from 0 to 120°. This calculation shows that the contribution of the Delbrück scattering to the total elastic cross section is small (about 10%) at 1.3 MeV. The γ -ray energies of the present experiment are below the threshold for pair production. The only contribution of the Delbrück scattering can therefore arise from the dispersive part since the absorptive part of the scattering amplitude vanishes at the threshold for pair production. Since the dispersive Delbrück amplitude decreases below the threshold for pair production^{11,12} while the Rayleigh amplitude increases, the Delbrück scattering can be neglected for the energies of the present experiment. The following consideration can therefore be restricted to Rayleigh scattering and Thomson scattering.

We write the cross section for elastic scattering in terms of circularly polarized waves. Let A denote the scattering amplitude for elastic scattering without changing the state of circular polarization (no spin flip) and A' the amplitude for scattering with change of the state of circular polarization then the cross section for elastic scattering is

$$d\sigma/d\Omega = r_0^2 [|A|^2 + |A'|^2], \quad (1)$$

where $r_0 = 2.818 \times 10^{-13}$ cm is the classical electron radius. A and A' can be represented as the sums of five terms

$$A = A_K + A_L + A_M + A_N + A_T, \quad (2)$$

$$A' = A'_K + A'_L + A'_M + A'_N + A'_T. \quad (3)$$

A_K , etc., are the amplitudes for Rayleigh scattering by K , L , M , N electrons, respectively. A_T and A'_T denote the Thomson scattering amplitudes. Rayleigh scattering from the O and P shell can be neglected for the energies and scattering angles considered in this paper.

The Rayleigh scattering from K electrons has been calculated by Brown *et al.*¹⁻⁴ To obtain good estimates of the Rayleigh amplitudes for the other shells and for the Z dependence of the K shell amplitudes, use was made of the observation by Brown *et al.*¹⁻⁴ that for low energies

(163 keV) the form-factor amplitudes¹³ agree fairly well with the dispersive parts of the scattering amplitudes, i. e., that

$$\text{Re}(A_K) \approx f_K (\cos\theta + 1)/2, \quad (4)$$

$$\text{Re}(A'_K) \approx f'_K (\cos\theta - 1)/2, \quad (5)$$

and that for higher energies (654, 1308 keV) a "corrected form factor" (Ref. 4)

$$g_K = \omega \int |\psi|^2 e^{i\Delta\vec{k} \cdot \vec{r}} [mc^2/(E+V)] d^3r \quad (6)$$

(ω : number of electrons in the shell, $\hbar\Delta\vec{k}$: momentum transfer, E : energy of the bound electron, $-V$: Coulomb potential) gives a good approximation of the no-spin-flip amplitude while f'_K still is a good approximation for the spin-flip amplitude.

The procedure in calculating the differential cross section was then to first adjust the numerical K -shell results of Brown *et al.*¹⁻⁴ to the γ energies and the $Z(=82)$ of this experiment. This was done by using the Z dependence indicated by f_K or g_K , and observing that the scattering amplitudes for a given scattering angle exhibit an almost linear energy dependence on a semi-logarithmic plot.

Following the procedure indicated by Brown *et al.*,⁴ the L -shell amplitudes for $E_\gamma = 279, 412$, and 662 keV were calculated according to

$$A_L = \text{Re}(A_K) g_L / g_K, \quad (7)$$

$$A'_L = \text{Re}(A'_K) f'_L / f'_K. \quad (8)$$

For $E_\gamma = 145$ keV Eq. (7) was modified by inserting f'_L/f'_K instead of g_L/g_K while Eq. (8) remained unaltered.

The form factors f_K, f_L, g_K, g_L were calculated using Dirac wave functions. For the M and N shells the nonrelativistic Hartree-Fock-Slater¹⁴ wave functions can be expected to give a useful description of the electronic configurations since they take into account the screening of the nuclear charge and since the contributions to the Rayleigh cross section arising from the M and N shells are significant only at relatively small momentum transfer. These wave functions were therefore used to calculate the form factors f_M and f_N and thus to approximate the scattering amplitudes analogous to the Eqs. (4) and (5).

The amplitudes for nuclear Thomson scattering are given by

$$A_T = Z^2(m/M)(\cos\theta + 1)/2, \quad (9)$$

$$A'_T = Z^2(m/M)(\cos\theta - 1)/2, \quad (10)$$

where Z is the charge number and m/M the ratio of electron and nuclear mass. The nuclear Thomson scattering is significant at large angles for the energies 662 and 412 keV.

IV. DISCUSSION

The results of experiment and calculation are compared in Fig. 4. The solid lines represent the cross sections calculated according to the method described above. The agreement with the experimental values is good except for the energy 145 keV.

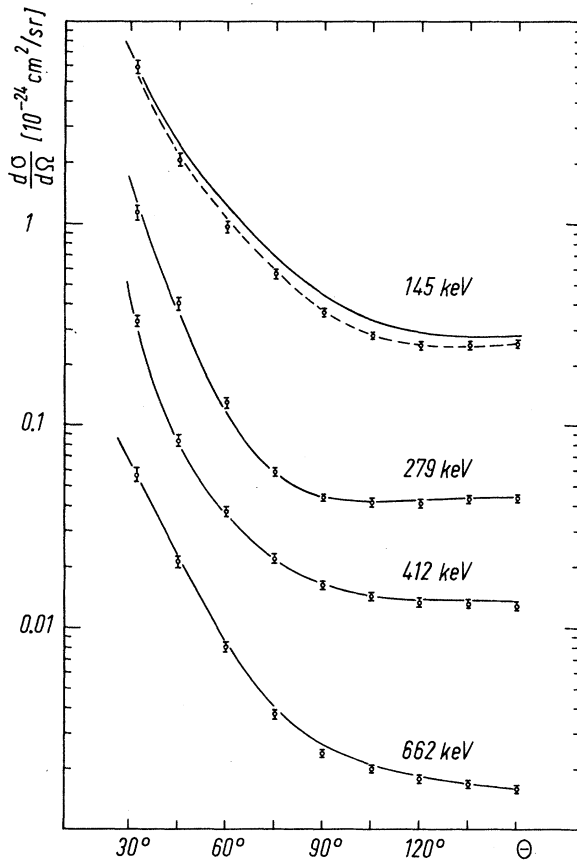


FIG. 4. Differential cross section for elastic scattering from lead versus scattering angle. The solid lines are calculated from the K -shell amplitudes given by Brown *et al.*¹⁻⁴ and from form factors for the L shell, calculated from unscreened relativistic wave functions. The dashed curve at 145 keV is obtained by applying a screening correction to the wave functions of the L electrons. In all cases corrections for Thomson scattering and Rayleigh scattering from the M and N shell are included.

As far as the discrepancy for the 145-keV γ radiation is concerned, it should be remembered that hydrogen-like relativistic wave functions were used for the calculation of the L -shell scattering amplitudes. These wave functions do not take into account the screening of the nuclear charge. The screening would have its largest influence on the cross section at the smallest γ energy since the contribution of the L shell to the cross section is largest and the effect of screening is expected to decrease rapidly with increasing momentum transfer. In order to see how large the screening effect might be for $E_\gamma = 145$ keV, f_L was recalculated using an estimated screening correction for the Dirac wave function. This correction was obtained by comparing the Schrödinger wave function with the nonrelativistic Hartree-Fock-Slater¹⁴ wave function. This calculation yielded the dashed curve in Fig. 4 which is in good agreement with the experiment. This rough approximation of a screening correction can only give to some extent reliable results for small momentum transfer, where the integration averages over large portions of the radial wave function. For this reason, and because of the expected decrease of the influence of the screening on the cross section with increasing momentum transfer, the recalculation of the L -shell form factors was not extended to higher energies.

The cross-section calculation given above was based on the assumption of in-phase coherence between Rayleigh and nuclear Thomson scattering and led to a good agreement with the experiment. This is in line with a theoretical consideration given by Moon,¹⁵ Dixon and Storey,⁵ on the other hand, found that the assumption of in phase coherence between Rayleigh and nuclear Thomson scattering led to a poor agreement between calculated and experimental cross sections for $E_\gamma = 1173$ and 1332 keV and a Pb scatterer while the assumption of incoherence led to a considerable improvement of the agreement. Furthermore, they found that an excellent agreement between experimental and calculated values could be achieved by describing the scattering process in terms of linearly polarized waves and assuming that A_R'' (the amplitude for Rayleigh scattering of waves which are polarized in the plane of scattering) is 180° out of phase with A_T'' , while A_R^\perp and A_T^\perp remain in phase. We, however, obtain for $E_\gamma = 662$ keV and $\theta = 150^\circ$ a discrepancy of about 25% between calculated and experimental cross sections by using the phase relations between Rayleigh and Thomson scattering proposed by Dixon and Storey.⁵

Since the K -shell amplitudes can be approximated by the Eqs. (4) to (6) it seemed to us of interest to investigate to what extent the differential cross section for elastic scattering can be represented by an expression of the form

$$\frac{d\sigma}{d\Omega} = r_0^2 \left\{ f^2 \left(\frac{\cos\theta + 1}{2} \right)^2 + f'^2 \left(\frac{\cos\theta - 1}{2} \right)^2 \right\} \quad (11)$$

with f and f' depending only on the momentum transfer and representing the amplitudes for scattering without and with spin flip. This formula converges to the former expression^{13,15}

$$d\sigma/d\Omega = r_0^2 F^2(1 + \cos^2\theta)/2 \quad (12)$$

in the limit $f = f' = F$. The functions f and f' can easily be derived from the measured differential cross sections since the regions of momentum transfer covered by the different γ -ray energies for scattering angles between 30 and 150° overlap to a large extent. We included in this calculation also the cross sections for 1173 and 1332 keV given by Dixon and Storey.⁵

In Fig. 5 the regions of momentum transfer covered by the different energies for θ between 30 and 150° are indicated by horizontal bars. The circles indicate the experimental values for f and f' . The curves b and c represent the form factors g_K and f_K , respectively. These curves show between $\lambda^{-1} \sin\theta/2$ of about 12 and

40 \AA^{-1} reasonable agreement with the experiment although one should expect that because of the neglect of the L -shell contribution they should be too small. The reason for the agreement is that both g_K and f_K are in the average too large in comparison to the exact scattering amplitudes of Brown *et al.*¹⁻⁴ This compensates approximately for the neglect of the L -shell contribution.

The curves d and e represent $g_K + Z^2m/M$ and $f_K + Z^2m/M$, respectively, indicating the contribution of the Thomson scattering to the elastic-scattering amplitudes. Curve e is in agreement with the experimental values while curve d is too high, indicating that g_K is too large at large momentum transfer. The general trend of the curves indicates that for momentum transfers larger than about 60 \AA^{-1} the Thomson amplitude alone is in agreement with the no-spin-flip scattering amplitude.

Brown *et al.*⁴ give an upper limit for the usefulness of g_K . This limit is, in our notation,

$$\lambda^{-1}(\sin\theta/2) = (41 \text{\AA}^{-1}) Z\alpha,$$

which is equal to 25 \AA^{-1} for $Z = 82$. Figure 5 shows that g_K might be used up to momentum

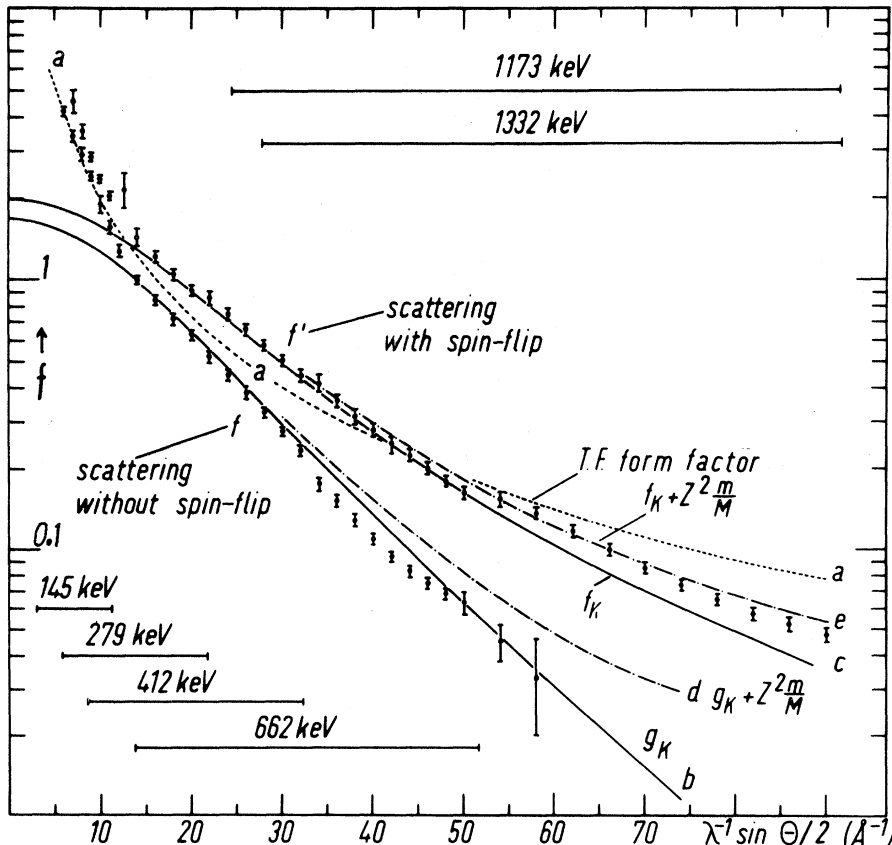


FIG. 5. Form factors versus momentum transfer. f and f' : experimental form factors for elastic scattering without and with spin flip, respectively. Curve a: Thomas-Fermi form factor. Curve b: "Corrected form factor" from relativistic K -shell wave functions. Curve c: form factor from relativistic K -shell wave functions. Curve e: Sum of curve a and the contribution Z^2m/M from Thomson scattering. Curve e: Sum of curve c and Z^2m/M .

transfers of 1.5 or 2 times the upper limit. For higher momentum transfers it is more adequate to set f equal to zero than equal to g_K . Fortunately this uncertainty does not affect the cross sections for large scattering angles too seriously since they are mainly determined by the amplitude for scattering with spin flip.

For practical purposes it is useful to know that f_K can be represented by the formula

$$f_K = \frac{2Z\alpha mc \sin[2\gamma \arctg(q/2Z\alpha mc)]}{\gamma q[1 + (q/2Z\alpha mc)^2]^\gamma} \quad (13)$$

with $\gamma = (1 - \alpha^2 Z^2)^{1/2}$ and q the momentum transfer. This formula was first given by Bethe and appears in papers by Levinger¹⁶ and Brown and Woodward.¹⁷

Curve a in Fig. 5 represents the form factor F calculated on the basis of the Thomas-Fermi

model.^{13,15} This form factor yields an adequate description of the differential cross section for Rayleigh scattering at very small momentum transfer, where scattering from the L shell and higher shells gives the main contribution.

Instead of the Thomas-Fermi model the non-relativistic Hartree-Fock model^{18,19} may be used for the calculation of F which was found^{20,21} to yield a slightly better representation of the cross section for Rayleigh scattering at very small momentum transfer.

ACKNOWLEDGMENTS

The author wishes to express his gratitude to Dr. F. R. Metzger for his encouraging interest in this work and for many valuable suggestions and discussions, and to Dr. J. Weiss, who did part of the computer programming.

*Work supported by the U. S. Atomic Energy Commission.

†Present address: II. Physikalisches Institut, Goettingen, Germany.

¹G. E. Brown, R. E. Peierls, and J. B. Woodward, Proc. Roy. Soc. (London) **A227**, 51 (1955).

²Sheila Brenner, G. E. Brown, and J. B. Woodward, Proc. Roy. Soc. (London) **A227**, 59 (1955).

³G. E. Brown and D. F. Mayers, Proc. Roy. Soc. (London) **A234**, 387 (1956).

⁴G. E. Brown and D. F. Mayers, Proc. Roy. Soc. (London) **A242**, 89 (1957).

⁵W. R. Dixon and R. S. Storey, Can. J. Phys. **46**, 1153 (1968).

⁶R. D. Evans, *Handbuch der Physik*, edited by S. Flügge (Springer-Verlag, Berlin, Germany, 1958), Vol. 34, p. 284.

⁷K. G. Standing and J. V. Jovanovich, Can. J. Phys. **40**, 622 (1962).

⁸J. Randles, Proc. Phys. Soc. (London) **A70**, 337 (1957).

⁹J. S. Levinger, Phys. Rev. **84**, 523 (1951).

¹⁰F. Ehlötzky and G. C. Sheppy, Nuovo Cimento **33**, 1185 (1964).

¹¹F. Rohrlich and R. L. Gluckstern, Phys. Rev. **86**, 1 (1952).

¹²H. A. Bethe and F. Rohrlich, Phys. Rev. **86**, 10 (1952).

¹³W. Franz, Z. Physik **98**, 314 (1935).

¹⁴F. Herman and S. Skillman, *Atomic Structure Calculations* (Prentice-Hall, Inc., Englewood Cliffs, New Jersey, 1963).

¹⁵P. B. Moon, Proc. Phys. Soc. (London) **A63**, 1189 (1950).

¹⁶J. S. Levinger, Phys. Rev. **87**, 656 (1952).

¹⁷G. E. Brown and J. B. Woodward, Proc. Phys. Soc. (London) **A65**, 977 (1952).

¹⁸A. T. Nelms and J. Oppenheim, J. Res. Natl. Bur. Std. (U.S.) **55**, 53 (1955).

¹⁹H. P. Hanson, F. Herman, J. D. Lea, and S. Skillman, Acta Cryst. **17**, 1040 (1964).

²⁰U. Hauser and B. Mussgnug, Z. Physik **195**, 252 (1966).

²¹A. Nath and A. M. Ghose, Nucl. Phys. **57**, 547 (1964).